

CONTINUOUS SEPARATION OF WHITE BLOOD CELL FROM BLOOD IN A MICROFLUIDIC DEVICE

Florina S. ILIESCU¹, Andreea P. STERIAN², Elena BARBARINI³, Marioara AVRAM⁴, Ciprian ILIESCU⁵

Articolul prezintă o metodă magnetoforetică de separare a celulelor albe ale sângeului prin curgere continuă pe cip. Separarea celulelor roșii din sânge este realizată folosind metoda unui gradient ridicat al câmpului magnetic pentru captarea în interiorul dispozitivului a acestor particule. Dispozitivul este realizat printr-o tehnologie de microfabricație și permite captarea celulelor roșii ale sângeului fără a folosi tehnici cunoscute. Metoda constă în curgerea probei diluate de sânge printr-un canal microfluidic unde un strat feromagnetic este supus permanent unui câmp magnetic exterior. Majoritatea celulelor roșii ale sângeului sunt captate în partea inferioară a dispozitivului în timp ce restul sănghelui este antrenat spre ieșire. Rezultatele experimentale arată că în medie 95% din celulele roșii sunt captate în dispozitiv.

This paper presents a magnetophoretic separation method on a chip of white blood cells from blood under continuous flow. The separation of red blood cells from the whole blood is performed using a high gradient magnetic separation method under continuous flow to trap the particles inside the device. The device is fabricated by microfabrication technology and enables to capture the red blood cells without the use of labeling techniques such as magnetic beads. The method consists of flowing diluted whole blood through a microfluidic channel where a ferromagnetic layer, subjected to a permanent magnetic field, is located. The majority of red blood cells are trapped at the bottom of the device while the rest of the blood is collected at the outlet. Experimental results show that an average of 95 % of red blood cells is trapped in the device.

Keywords: microfluidics, continuous flow, blood, paramagnetic separation

¹M.D, Republic Polytechnic, Singapore

²PhD, Dept. of Physics, University POLITEHNICA of Bucharest, Romania

³PhD student, Politecnico di Torino, Electronics Department, Italy

⁴PhD, National Institute for Research and Development in Microtechnologies, Romania, e-mail: marioara.avram@imt.ro

⁵PhD., Institute of Bioengineering and Nanotechnology, Singapore, e-mail: ciliescu@ibn.a-star.edu.sg

1. Introduction

Micro total analysis systems (μ TAS) and laboratories-on-a-chip is one of the key growth industries in the future due to its small sizes, easy to use, transportability and sure due to the small amount of the sample required to be analyzed [1,2]. Manipulation and characterization of small quantities of biological samples are some of the targets on lab on chip devices.

One approach is using electric field – dielectrophoresis –for cell trapping [3-6] or cell separation [7-10] or even for electrofusion of small lipid containers – liposome- [11]. Main disadvantages are related to the huge electric field gradient which can generate an increase temperature gradient (in spite of the existing solution for a limitation of Joule effect [12]), and the fact that, not always, the dielectric properties of the cells allowed separation of two or more populations.

Another solution can be using magnetic field: immunomagnetic (cell separation in which magnetic particle are selectively attach to cell beads [13-15]) which can be a very performing method especially for separation of rare cell types. Other research [16-19] use targets the native magnetic properties of some biological cells (deoxyhemoglobin red blood cells). Separation of red blood cells from whole blood is often an essential step before the application of many clinical and molecular diagnostic tests on blood samples. The procedure is also useful in blood transfusion applications as it allows the selective transfusion of particular cell types. Separation can be possible due to hemoglobin. Hemoglobin is a conjugated metal-protein comprising of four polypeptide globins chains containing a ring structure covalently bonded with a central ferrous iron atom (Fe^{2+}), which binds reversibly with oxygen. If is deoxygenated, each of the four iron atoms contains four unpaired electrons, giving the protein and the cell a substantial paramagnetic moment. White blood cells do not contain hemoglobin and are diamagnetic particles. These properties are the starting point for the red blood cells trapping using high gradient magnetic separation.

This paper presents a simple microfluidic device for extraction of red blood cells from blood under continuous flow. The device consist in two glass dies: one with the inlet/outlet holes and the microfluidic channel, the other one with “dots” of ferromagnetic layer. The geometry of the ferromagnetic layer and the application of an external permanent magnetic field perpendicular to the flow direction generate a magnetic force on the red blood cells presented in the blood. The device also offers other advantages, such as the collection of the red blood cells inside the channel. Glass structure allows the complete visibility and analysis of the sample.

2. Design of the microfluidic device for magnetophoretic separation

The design of the device is relatively simple and involves glass microfabrication. A glass die with inlet / outlet holes and a 60 μm -depth microfluidic channel is bonded to another glass die, on which a ferromagnetic structure consisting off square “dots” (2x2x2 μm) of Ni (Figure 1). A permanent magnet generates a magnetic field perpendicular on the flow direction. The blood is diluted with PBS and is flown through the microfluidic channel. The ferromagnetic “dots” generate a gradient of magnetic field which amplifies the magnetic force that acts on red blood cells. As results the red blood cells (RBC) are trapped by the ferromagnetic layer while the white blood cells (WBC) are flushed out with the plasma and the other blood components.

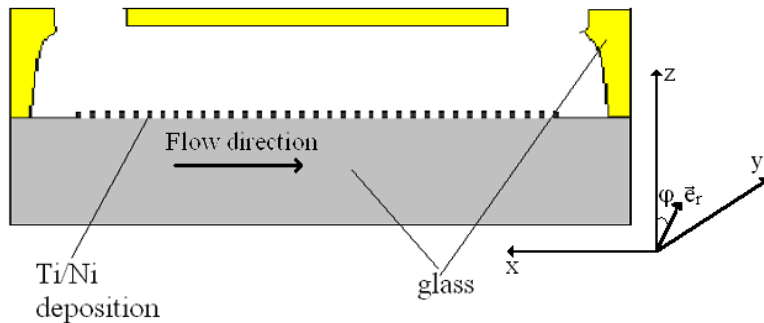


Fig. 1. Schematic view of the microfluidic device for separation of RBC and WBC

3. Separation principle

If a uniform external magnetic field is applied normal to the axis of a ferromagnetic wire, it is deformed near the ferromagnetic wire, and generates a high gradient magnetic field, experienced by the magnetic particles moving around the wire. Therefore, blood cells flowing near the ferromagnetic wire experience a magnetic force created by the high gradient magnetic field near the ferromagnetic rectangular wire, with w - width and h - height.

The magnetic force of a ferromagnetic wire on blood cells, located around the x-axis, can be calculated as [17]:

$$\vec{F}_{BC} = -\frac{2k\mu_0\Delta\chi \cdot V_{BC}a^2}{r^3} \left(k \left(\frac{w}{h} \right) \frac{a^2}{r^2} + \cos 2\varphi \right) \left(\frac{w}{h} \right) H_0^2 \vec{e}_r - \frac{2k\mu_0\Delta\chi \cdot V_{BC}a^2}{r^3} \left(\frac{w}{h} \right) H_0^2 \sin 2\varphi \vec{e}_\varphi, \quad r > a \quad (1)$$

with

$$k = \frac{\mu_w - \mu_B}{\mu_w + 2 \cdot \mu_B}, \quad M_S = k H_0 \quad (2)$$

where $\Delta\chi = \chi_{BC} - \chi_B$ is the relative magnetic susceptibility of a blood cell relative to the buffer solution; μ_w and μ_B are the magnetic permeabilities of the ferromagnetic layer and the buffer solution, respectively; V_{BC} is the volume of the blood cell; a is the lateral dimension of the ferromagnetic structure; r and φ are the cylindrical coordinates of the distance and angle; H_0 is the external magnetic field; and \vec{e}_r and \vec{e}_φ are unit vectors for the distance and angle in the cylindrical coordinate.

If the ferromagnetic structure is magnetically saturated, the first term of the magnetic force in equation (1) is independent of the external magnetic field, H_0 , and proportional to the square of the saturation magnetization. The second and third terms of the magnetic force are linearly proportional to the product of the saturation magnetization M_s and the external magnetic field H_0 .

For magnetic particles placed (approximately) on the z-axis ($\varphi \approx 0$ in Figure 1), $\sin 2\varphi \approx 0$, $\cos 2\varphi \approx 1$, the ferromagnetic material attracts paramagnetic particles (red blood cells) and repels diamagnetic particles (white blood cells). For magnetic particles placed on the y-axis ($\varphi \approx 90$), $\sin 2\varphi \approx 0$, $\cos 2\varphi \approx -1$, the material attracts diamagnetic particles (white blood cells) and repels paramagnetic particles (red blood cells). The first geometric configuration has been called the paramagnetic capture mode; the later has been called the diamagnetic capture mode. Therefore, to achieve a higher magnetophoretic force, the magnetophoretic microseparator is designed in the paramagnetic capture mode with a rectangular ferromagnetic structure.

To summarize, the main parameters that influence the magnetic force applied on the particles affected by an external magnetic field are: the intensity and orientation of the magnetic field H_0 ; the permeability of the buffer solution and the ferromagnetic material; the susceptibilities of the cells and the buffer solution and the dimension of the device.

4. The Fabrication process of the microfluidic device

Three major steps characterize the fabrication process of the microfluidic device for continuous separation of red blood cells and white blood cells:

- fabrication of the top wafer with the inlet/outlet holes and the microfluidic channel;
- fabrication of the bottom wafer with ferromagnetic concentrators;
- bonding of the wafers.

For the top wafer a 4" Pyrex glass wafer (Corning 7740) was chosen for the microfabrication process, mainly due to its good wet etching properties [20, 21]. The fabrication process is summarized in Figure 2. For the etching of the microfluidic channel - Figure 2a- a Cr/Au/photoresist mask was used ([22]). The

Cr/Au (50 nm/500 nm) layer was deposited on a CHA e-beam evaporator, the Au layer being deposited in 3 steps in order to cover the deposition defects ([22]). The patterning of the Cr/Au was performed using a 2 μ m-thick photoresist mask (AZ7220 from Clariant) and classical Au and Cr wet etchants. In order to increase the hydrophobicity of the masking layer, recommended for deep wet etching process in high concentrated HF solution [23], the photoresist was hard backed at 120°C for 30 minutes on a hot plate. The wet etching process (Figure 2b) was performed in HF (49%) /HCl (37%) in ratio 10/1, optimized in [24]. This etching

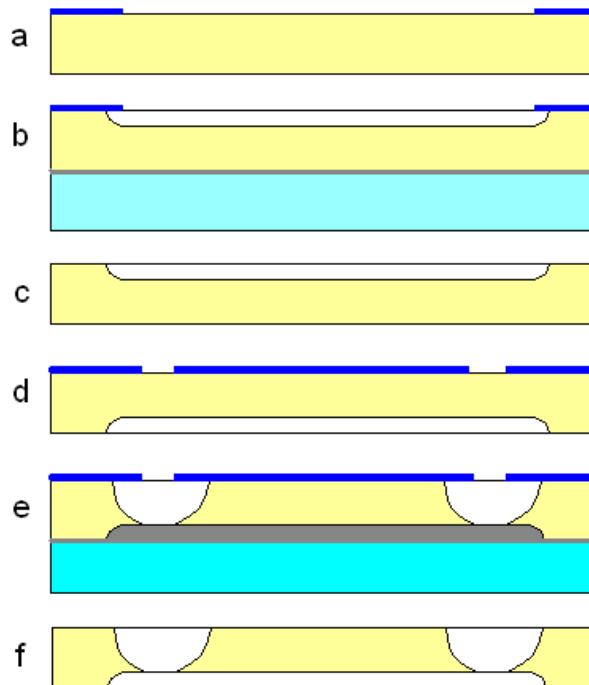


Fig. 2. Main steps of the fabrication process of the top wafer: a) processing of the Cr/Au/photoresist masking layer, b) wet etching of the microfluidic channel, c) removing of the masking layer, d) processing of the Cr/Au/photoresist masking layer for inlet/outlet holes, e) wet etching of inlet/outlet holes, f) removing of the second masking layer.

solution assures a fast etching rate (7.5 μ m/min) as well as a good roughness of the generated surface ($R_a = 3$ nm). HCl removes the insoluble products resulted after the reaction of Al_2O_3 (present in the glass composition) with HF. The etch depth was 60 μ m (performed during 8 minute in a Teflon container using magnetic stirring). During the wet etching process the backside of the wafer was protected by a dummy silicon wafer bonded with wax on the glass wafer. The wax bonding and debonding process was performed on a hot plate. After removing of the Cr/Au/photoresist mask (Fig. 2c) using classical resist stripper (NMP) – for photoresist and residual wax and Au and Cr etchants, a second Cr/Au/photoresist

mask was applied on the opposite surface of the glass wafer (Fig. 2d). The thickness of the deposited Au layer was $1\mu\text{m}$, due to the fact that the required depth of the etching process was increased (around $440\mu\text{m}$). The preparation of the mask was similar with the process described for the generation of the microfluidic channel. Similar, a second wax bonding process will assure the protection of the microfluidic channel, while the wax served also as etch-stop layer for the deep wet etching process in same HF/HCl (Fig. 2e). The etching time was 70 minutes (over etch for compensation of the nonuniformity of the etching process). Finally, the glass wafer was debonded from the dummy silicon wafer and the masking layer was removed with a similar procedure as was described before.

The fabrication of the bottom wafer consists of a simple lift off process presented in Fig. 3. On a similar 4" glass wafer (Corning 7740) a $5\mu\text{m}$ -thick photoresist mask (AZ4620 from Clariant) was deposited (Fig. 3a) followed by a descum process (1min) on a RIE system using oxygen. The metal layer Ti/Ni ($50\text{ nm}/2\mu\text{m}$) was deposited in a CHA e-beam evaporator – (Fig. 3b). The photoresist masking layer was finally removed in an ultrasonic bath using acetone.

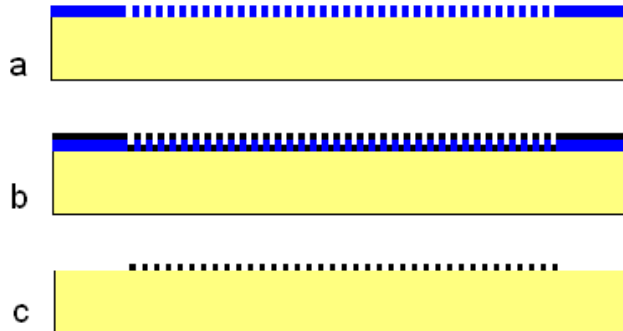


Figure 3: Main steps of the bottom wafer fabrication process: a) deposition of the photoresist mask, b) deposition of Ti/Ni layer, c) removing of the photoresist mask.

The bonding of the glass wafers was performed using a simple adhesive bonding with SU8-5 photoresist [25, 26]. This technique was preferred to other methods such as: glass fusion bonding described by Saarela *et al* [27] or adhesive bonding using parylene previously used in [28, 29] for other applications. The technique consists of imprinting of an SU8-5 layer initially spun on a dummy silicon wafer (Fig. 4a) on a Teflon cylinder (Fig. 4b) and of transferring further the adhesive from the cylinder to the top glass wafer (Fig. 4c). This contact imprinting technique allowed deposition of a thin adhesive layer only on the bonding regions. In the last step, the wafers are manually align and bonded at 150°C for 30 minutes with an applied pressure of 1000 N (Fig. 4d). Finally, the wafer

is diced. An image of the fabricated device is presented in Fig. 5. The dimensions of the chip are 32 mm x 9 mm.

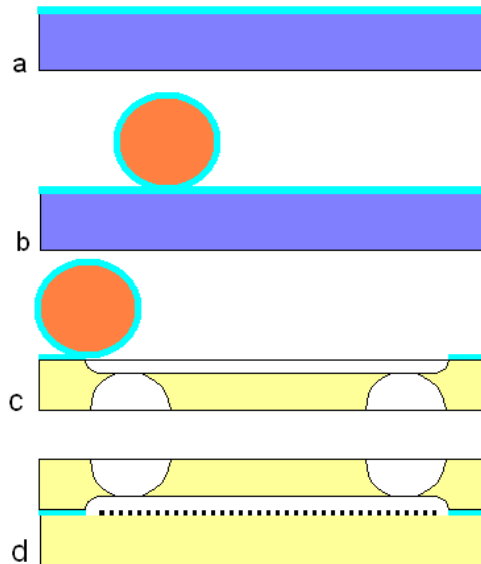


Fig. 4. Adhesive bonding of the glass wafers using contact imprinting method:

- spinning the SU8 on a dummy (silicon) wafer,
- imprinting of the adhesive (SU8) on a Teflon cylinder from the dummy wafer
- transferring the adhesive layer on the glass surface
- bonding

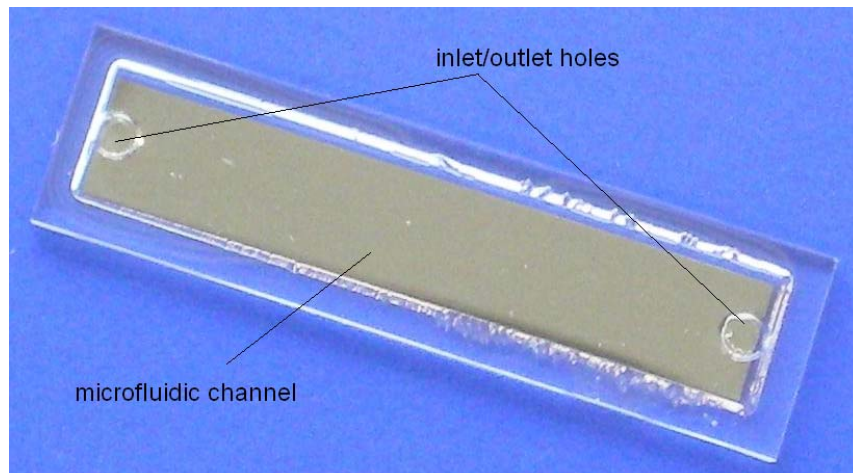


Fig. 5. Image with the fabricated microfluidic device for magnetophoretic separation of red blood cells and white blood cells

5. Testing

Diluted blood (1:20 in PBS) was used for testing purpose. The permanent magnet creates an external magnetic flux density (magnetic induction) of 0.2 T and the flow rate was set in the range between 0.5 and 0.7 ml/h (using a syringe pump). Two connectors fabricated by polymer printing secured the inlet and outlet connections. The results are based on the quantitative analysis of the red cells collected at the output of the device. Experimental results show an average of 5% of red blood cells collected at the output of the device. Fig. 6 presents the image with the field densities of cells before and after the sample was flown through the microfluidic device.

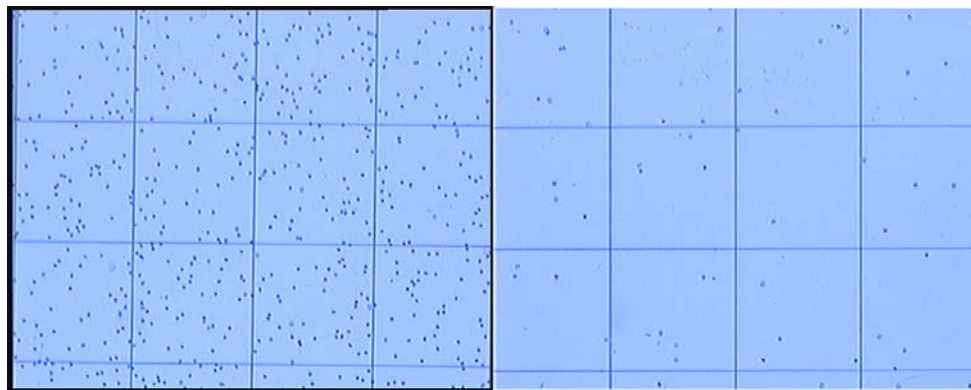


Fig. 6. Image of the field density of the cells on Neubauer hemocytometer before and after flowing the blood sample through the microfluidic device

6. Conclusions

The paper presents a microfluidic device for magnetophoretic trapping of red blood cells under continuous flow, using high gradient of magnetic field. Experimental results show a good trapping efficiency that can be further improved.

R E F E R E N C E S

- [1] *J. West, M. Becker, S. Tombrink, and A. Manz*, “Micro total analysis systems: Latest achievements,” *Anal. Chem.*, vol. 80(12), (2008) pp. 4403-4419.
- [2] *P.A. Abgrall, and A.M. Gué*, “Lab-on-chip technologies: making a microfluidic network and coupling it into a complete microsystem—a review,” *J. Micromech. Microeng.*, vol. 17(5), (2007) pp. R15-R49.
- [3] *C. Iliescu, G.L. Xu, F.E.H. Tay, and V.D. Samper*, “Dielectrophoretic chip with bulk Silicon electrodes” *Proc. SPIE*, vol. 5651, (2005) pp. 254-264.

- [4] *C. Iliescu, G.L. Xu, F.C. Loe, P.L. Ong, and F.E.H. Tay*, “A 3 dimensional dielectrophoretic filter chip”, *Electrophoresis*, vol. 28(7), (2007) pp. 1107-1114.
- [5] *L. Wang, L.A. Flanagan, N.L. Jeon, E. Monuk, and A.P. Lee*, “Dielectrophoresis switching with vertical sidewall electrodes for microfluidic flow cytometry,” *Lab Chip*, vol. 7(9), (2007) pp. 1114-1120.
- [6] *Y.T. Zhang, F. Bottausci, M.P. Rao, E.R. Parker, I. Mezic and N.C. MacDonald*, “Titanium-based dielectrophoresis devices for microfluidic applications,” *Biomed. Microdev.*, vol. 10(4), (2008) pp. 509-517.
- [6] *C. Iliescu, F.E.H. Tay, G.L. Xu, and L.M. Yu*, “Cell separation technique in dielectrophoretic chip with bulk electrode,” *Proc. SPIE*, vol. 6036, (2005) 60360E.
- [7] *C. Iliescu, L.M. Yu, F.E.H. Tay and B.T. Chen*, “Bidirectional field flow particle separation method in a dielectrophoretic chip with 3D electrodes,” *Sens. Actuators B*, vol. 129 (1), (2008) pp. 491-496.
- [8] *C. Iliescu, G.L. Xu, and F.E.H. Tay*, “Sequential field-flow cell separation method in a dielectrophoretic chip with 3D electrodes,” *J. Microelectromech. Syst.*, vol. 16(5), (2007) pp. 1120-1129.
- [9] *Iliescu, C., Tresset, G. and Xu, G.L.*, “Continuous field-flow separation of particle populations in a dielectrophoretic chip with three dimensional electrodes,” *Appl. Phys. Lett.*, vol. 90(23), (2007) pp. 234104.
- [10] *Tresset, G. and Iliescu, C.*, “Electrical control of loaded biomimetic femtoliter vesicles in microfluidic system,” *Appl. Phys. Lett.*, vol. 9(17), (2007) pp.173901.
- [11] *F.E.H. Tay, L. Yu, A.J. Pang and C. Iliescu*, “Electrical and thermal characterization of a dielectrophoretic chip with 3D electrodes for cells manipulation,” *Electrochimica Acta*, vol. 52(8), (2007) pp. 2862-2868.
- [12] *Q. Ramadan, C. Yu, V. Samper and D.P. Poenaru*, “Microcoils for transport of magnetic beads,” *Appl. Phys. Lett.*, vol. 88(3), (2006) pp. 032501.
- [13] *Deng, T., Prentiss, M. and Whitesides, G.M.*, “Fabrication of magnetic microfiltration systems using soft lithography,” *Appl. Phys. Lett.*, vol. 80(3), (2002) pp. 461-464.
- [14] *D.W. Inglis, R. Riehn, R.H. Austin, and J.C. Sturm*, “Continuous microfluidic immunomagnetic cell separation,” *Appl. Phys. Lett.*, vol. 85(21), (2004) pp. 5093-5095.
- [15] *K. Han, and A.B. Frazier*, “Continuous magnetophoretic separation of blood cells in microdevice format,” *J. Appl. Phys.*, vol. 96, (2004) pp. 5797-5802.
- [16] *D.W. Inglis, R. Riehn, J.C. Sturm, and R.H. Austin*, “Microfluidic high gradient magnetic cell separation,” *J. Appl. Phys.*, vol. 99(8), (2006) pp. 08K101.
- [17] *K. Han, and A.B. Frazier*, “Paramagnetic capture mode magnetophoretic microseparator for high efficiency blood cell separations,” *Lab Chip*, vol. 6(2), (2006) pp. 265-273.
- [18] *J. Svoboda*, “Separation of red blood cells by magnetic means,” *J. Magn. Magn. Mater.*, vol. 220, (2000) pp. L103-L105.
- [19] *C. Iliescu, B.T. Chen, F.E.H. Tay G.L. Xu and J.M. Miao*, “Characterization of deep wet etching of glass,” *Proc. SPIE*, vol. 6037, (2006) pp. A370.
- [20] *C. Iliescu, B. Chen and J.M. Miao*, “On the wet etching of Pyrex glass,” *Sens. Actuators A*, vol. 143(1), (2008) pp.154-161.
- [21] *C. Iliescu, F.E.H. Tay, and J.M. Miao*, “Strategies in deep wet etching of Pyrex glass,” *Sens. Actuators A*, vol. 133(2), (2007) pp. 395-400.
- [22] *F.E.H. Tay, C. Iliescu, J. Jing, and J.M. Miao*, “Defect-free wet etching through Pyrex glass using Cr/Au mask,” *Microsyst. Technol.*, vol. 12, (2006) pp. 935-939.
- [23] *C. Iliescu, J. Jing, F.E.H. Tay, J. Miao and T.T. Sun*, “Characterization of masking layers for deep wet etching of glass in an improved HF/HCl solution,” *Surf. Coat. Tech.*, vol.198, (2005) pp.314-318.

- [24] *L. Yu, A.J. Pang, B.T. Chen, F.E.H. Tay, and C. Iliescu*, “Adhesive wafer-to-wafer bonding using contact imprinting,” Proc. SPIE, vol. 6415, (2007) pp. I4151.
- [25] *C. Iliescu, D.P. Poenar, M. Carp and F.C. Loe*, “A microfluidic device for impedance spectroscopy analysis of biological samples,” Sens. Actuators B, vol. 123(1), (2007) pp.168-176.
- [26] *V. Saarela, M. Haapala, R. Kostiainen, T. Kotiaho, and S. Franssila*, “Glass microfabricated nebulizer chip for mass spectrometry,” Lab Chip., vol. 7, (2007) pp.644-646.
- [27] *D.P. Poenar, C. Iliescu, M. Carp, A.J. Pang, and K.J. Leck*, “Glass-based microfluidic device fabricated by Parylene wafer-to-wafer bonding for impedance spectroscopy,” Sens. Actuators A, vol. 139, (2007) pp.162-171.
- [28] *H. Kim and K. Najafi*, “Characterization of low-temperature wafer bonding using thin-film parylene,” J Microelectromech. Syst., vol. 14(6), (2005) pp.1347–1355.
- [29] *A. Ciancio, V. Ciancio, F. Farsaci*, “ Wave propagation in media obeying a thermoviscoelastic model,” U.P.B. Sci. Bull., Series A, Vol. 69, No. 4, 2007 ISSN 1223-7027, pp.69-81.